On the value of relative flow data

van Erp, Paul B.C.; Knoop, Victor L.; Hoogendoorn, Serge P.

DOI
10.1016/j.trc.2019.05.001

Publication date
2020

Document Version
Final published version

Published in
Transportation Research Part C: Emerging Technologies

Transportation Research Part C 113 (2020) 74–90

Contents lists available at ScienceDirect

Transportation Research Part C

journal homepage: www.elsevier.com/locate/trc

On the value of relative flow data☆

Paul B.C. van Erp*, Victor L. Knoop, Serge P. Hoogendoorn

Delft University of Technology, Stevinweg 1, 2628 CN Delft, the Netherlands

ARTICLE INFO

Keywords:
Relative flow data
Cumulative flow
Traffic state estimation
Information assimilation
Learning models

ABSTRACT

Traffic flow can be described using three dimensions, i.e., space x, time t and cumulative flow N. This study considers estimating the cumulative flow over space and time, i.e., $N(x, t)$, using relative flow data collected by stationary and moving observers. Stationary observers, e.g., loop-detectors, can observe flow at fixed position over time. Furthermore, automated or other equipped and connected vehicles can serve as moving observers that observe flow relative to their position over time. To present the value of relative flow data, in this paper, we take the perspective of a model-based estimation approach. In this approach, the data is used in two processes: (1) information assimilation of real-time data and models and (2) learning of the models used in information assimilation based on historical data. This paper focuses on traffic state estimation on links. However, we explain that, in absence of stationary observer that are positioned at the link boundaries, it is valuable to consider the information propagation over nodes. Throughout this study a LWR-model with a triangular fundamental diagram (FD) is used to develop the principles that can be used for the two processes. These principles are tested in a simulation (VISSIM) study. This study shows that we can find the traffic flow model parameters and can partially estimate the link boundary conditions based on relative flow data collected by moving observers alone. It also shows that the traffic flow behavior differs partially from the LWR-model with triangular FD, and therefore, we recommend the option to learn and use other traffic flow models in future research. Overall, relative flow data is considered valuable to obtain model learning datasets and to estimate the traffic state.

1. Introduction

Traffic state estimation (TSE) is an important element in road traffic operations management and planning (Seo et al., 2017). It is, for instance, important in infrastructure planning, dynamic traffic management (DTM) systems and navigation services. For each application the desired estimation output can differ in terms of accuracy, reliability and semantics. For instance, navigation services and DTM systems require real-time information, while this time-constraint is not there for infrastructure planning applications. Furthermore, the required spatial resolution can differ, e.g., a local DTM system requires less spatial coverage than a navigation service that needs information for all elements on each potential route.

A road traffic network can be represented as a set of links (roads), nodes (intersections or discontinuities like lane drops) and network boundaries (source and sink nodes) (Seo et al., 2017). This paper focuses on TSE on links; however, as will be explained in this paper, information that propagates over a network of links and nodes can also be valuable for link TSE. Therefore, we will discuss

☆ This paper has been accepted for a podium presentation at the 23rd International Symposium on Transportation and Traffic Theory, ISTTT 23, 24–26 July 2019, Lausanne, Switzerland

* Corresponding author.
E-mail address: p.b.c.vanerp@tudelft.nl (P.B.C. van Erp).

https://doi.org/10.1016/j.trc.2019.05.001
Received 30 November 2018; Received in revised form 8 March 2019; Accepted 2 May 2019
Available online 28 May 2019

how information can propagate over such a network.

On a link, traffic flow can be described using three dimensions, i.e., space x, time t and cumulative flow N (Makigami et al., 1971). The cumulative flow $N(x, t)$ is defined as the number of vehicles that have passed location x at time t, where it is important that we include the same set of vehicles at all locations. If $N(x, t)$ is smoothed and continuously differentiable, the macroscopic traffic flow variables flow q, density ρ and mean speed u can be obtained by taken the derivatives of $N(x, t)$ to time and space. Furthermore, overall link properties, i.e., the link travel-time and link vehicle accumulation (number of vehicles on the link), can be obtained from the cumulative flow at the link boundaries, i.e., x_0 (upstream boundary) and x_L (downstream boundary). Due to large informative value of the cumulative flow, in this study, we focus on estimating $N(x, t)$ within a space-time domain.

This study presents the value of relative flow data for TSE. This variable (relative flow) describes the change in cumulative flow, i.e., ΔN, over a path in space-time (which we denote as an observation path). Automated or other equipped and connected vehicles could serve as moving observers that collect these data by observing the vehicles that they overtake and that overtake them (Redmill et al., 2011; Florin and Olariu, 2017; Van Erp et al., 2018a). Furthermore, stationary observers, e.g., loop-detectors or road-side camera-systems, can be used to observe the flow at a fixed position over time. For stationary observers the observation path is a horizontal line in space and time. Although both describe the flow relative to the observation path, only stationary observers consistently observe the macroscopic variable flow q.

To present the *value of data*, we take the perspective of a model-based estimation approach, see Fig. 1. In this approach, the data are used for two processes (which are highlighted using the blue[1] boxes): (1) Real-time data and models are fused, which we denote as information assimilation (IA), to estimate the traffic state. And, (2) historical data are used to learn the models that are used in IA. This study focuses on explaining the principles that can be used for both processes and how relative flow data can be transformed into valuable information using these principles. Therefore, the principles help us to understand why the characteristics of relative flow data (i.e., the combination of the observed variable and spatial-temporal characteristics) have a large value in traffic state estimation. Designing and testing full methodologies for the two processes, which are aimed at extracting the potential information in the data, is beyond the scope of this study.

Throughout this study, we consider data scenarios that rely on a combination of stationary and moving observers, and that rely on moving observers alone. Positioning stationary observers at the link boundaries aligns with existing studies, e.g., Claudel and Bayen (2010a) and Sun et al. (2017), as the resulting boundary observations play a crucial role in the estimation of $N(x, t)$. However, multiple studies opt to limit the dependence of these stationary observers due to the high installation and operation costs (Seo et al., 2017). Therefore, we will focus on scenarios in which we solely rely on moving observers to collect the relative flow data.

The main contributions of this paper are: (1) We show which valuable information relative flow data provide to learn the link traffic flow model. For this purpose, we first explain which learning dataset can be constructed using relative flow data and then explain which informative value this dataset has to find the model parameters. (2) We show how relative flow data can be fused with the link traffic flow model to connect observation paths, estimate the link boundary conditions, and estimate the link supply and demand. These principles can be used to estimate the traffic state based on moving observers alone. Furthermore, we explain that, in absence of stationary observers that are positioned at the link boundaries, it may be valuable to consider information propagation over nodes and that the estimates (i.e., link boundary conditions, supply and demand) may be used for this purpose. (3) Based on these principles, we explain why it is valuable to observe the change in cumulative flow using observers that travel at different speeds with respect to each other and with respect to the characteristic wave speeds of the link traffic flow model.

This paper is organized as follows. In Section 2, the potential relative flow data characteristics are discussed are compared to other data types. Section 3 explains why the relative flow data are valuable in the two processes that are part of the model-based estimation approach. In that section, different principles are explained that can be used to learn the link traffic flow model and estimate the cumulative flow over space and time. To test and provide a better understanding of these principles, a simulation (VISSIM) case study was conducted and is presented in Section 4. Finally, the conclusions are presented in Section 5.

Throughout this paper many different symbols are used. A description of these symbols is provided in Table 1.

2. Collecting relative flow data with stationary and moving observers

This section discusses the potential characteristics of relative flow data. We make a distinction between data collected with stationary observers and data collected with moving observers. The former are collected with road-side sensing equipment, e.g., loop-detectors (Treiber and Helbing, 2002; Wang and Papageorgiou, 2005; Van Hinsbergen et al., 2012). The latter may be collected with vehicles equipped with sensors that observe the other road-users (Redmill et al., 2011; Florin and Olariu, 2017; Van Erp et al., 2018a,b).

Below, we first discuss the potential characteristics of relative flow data that are collected with stationary or moving observers (Section 2.1). Next, Section 2.2 discusses which types of data are used in studies that propose methodologies that estimate the traffic state in or via the cumulative flow plane.

2.1. Potential data characteristics

Stationary and moving observers both observe the flow relative to a path in space-time. We refer to this path as the observation

[1] For interpretation of color in Figs. 1, 6, 7, 11, 12, the reader is referred to the web version of this article.

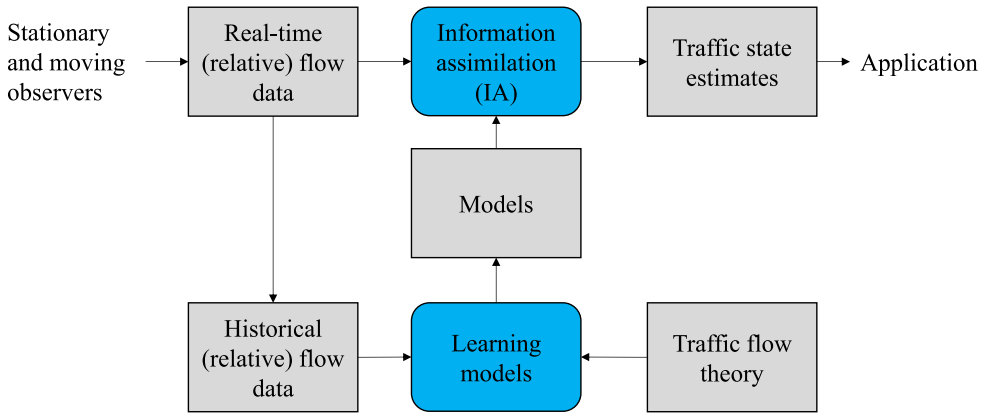

Fig. 1. Schematic representation of the considered model-based estimation approach.

Table 1
Description of symbols that are used in this article.

Description	Notation	Unit
Position	x	m
Time	t	s
Location upstream link boundary	x_0	m
Location downstream link boundary	x_L	m
Flow	q	veh/s
Density	ρ	veh/m
Mean speed	u	m/s
Cumulative flow	N	veh
Position of observer o at time t	$X_o(t)$	m
Speed of observer o at time t	$V_o(t)$	m/s
Cumulative flow on the observation path of observer o at time t	$N_o(t)$	veh
Time when observer o is at position x	$T_o(x)$	s
Triangular fundamental diagram:		
Free-flow speed	v^f	m/s
Wave speed	w	m/s
Passing rate	r	veh/s
Capacity	q^C	veh/s
Critical density	ρ^{cr}	veh/m
Jam density	ρ^j	veh/m
Newell's method:		
Boundary over which the cumulative flow is known	$\mathcal{B}$	
Space-time point for which the cumulative flow is estimated	P	
Change in cumulative flow over v^f-wave from $\mathcal{B}$ to P	$\Delta N^{\text{ff}}_{\mathcal{B}P}$	veh/s
Change in cumulative flow over w-wave from $\mathcal{B}$ to P	$\Delta N^{\text{cg}}_{\mathcal{B}P}$	veh/s
Speed of potential characteristic waves	v^c	m/s
Model parameter p guess	$\hat{p}$	*Depends on parameter*
Error in model parameter guess	ε	*Depends on parameter*
Error in element of Eq. (4)	Υ	m/s
Supply	S	veh/s
Demand	D	veh/s
Upper bound restriction of the cumulative flow	$\tilde{N}^+$	veh
Lower bound restriction of the cumulative flow	$\tilde{N}^-$	veh

path. The position and speed of observer o at time t are respectively given by $X_o(t)$ and $V_o(t)$, where $V_o(t) = \partial_t X_o(t)$. The observation path of a stationary observer is a horizontal line in the space-time plane, i.e., it observes the flow with respect to a fixed position over time. Moving observers observe the flow with respect to their position over time, i.e., their trajectory. Depending on the sensing equipment and the infrastructure moving observers may also observe the flow for the traffic flow in the other direction. In this case, the moving observer is not part of the traffic in the direction of interest and moves with a negative speed through space-time. Fig. 2 shows the observation paths for stationary observers, and moving observers that are part of the traffic flow or move in opposing direction. The observer speeds of these types of observers will respectively be $V_o(t) = 0$, $V_o(t) \geqslant 0$ and $V_o(t) \leqslant 0$.

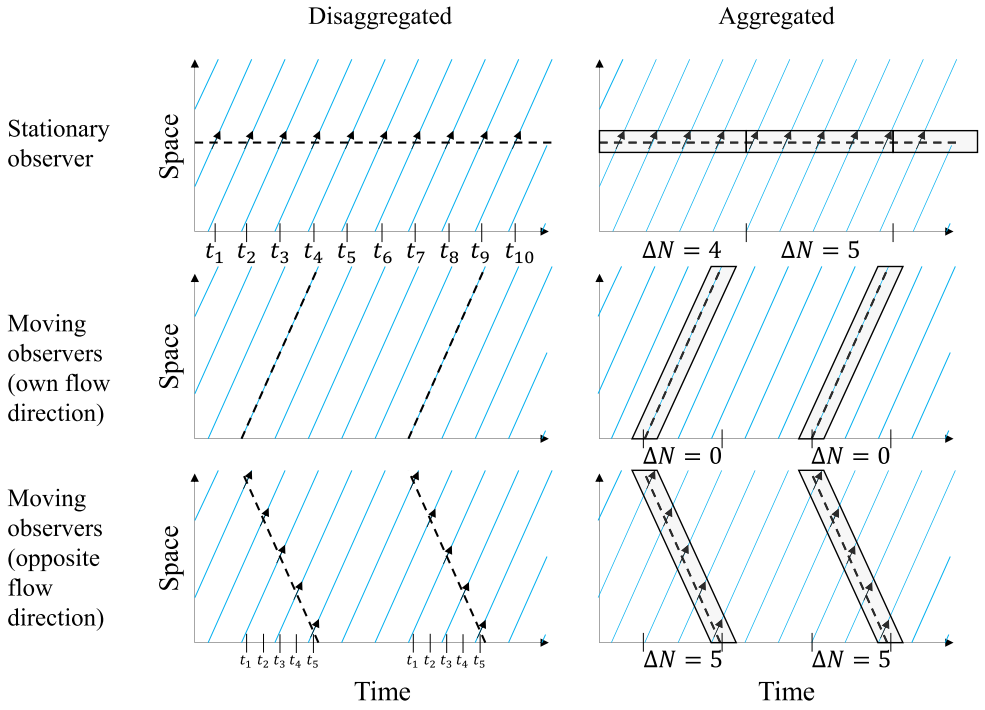

Fig. 2. Aggregation level and spatial-temporal characteristics of (relative) flow data collected by different observers.

Traffic sensing data can be disaggregated or aggregated (Seo et al., 2017). We solely use this categorization to define the flow data. Disaggregated flow data describe all individual passings, i.e., time and direction. For stationary observers the direction is always the same, i.e., the vehicle overtakes the stationary observer. In this case the cumulative flow N increases by one, i.e., $+1$. Moving observers that travel in flow direction can be overtaken by another vehicle (N increases by one) or overtake another vehicle (N decreases by one). Aggregated flow data describe the sum of all passings within a time-period. Fig. 2 visually shows the difference between disaggregated or aggregated relative flow data for the different observers.

The observation path for stationary observers is fixed. Therefore, information related to the passing (disaggregated) or flow (aggregated) suffices. However, spatial-temporal information, i.e., its position over time, is needed for moving observers. This information may be shared with a fixed time-interval (temporal-sampling), with a fixed space-interval (spatial-sampling), in case of an event, e.g., passing, or a combination of these options. If the flow data is disaggregated it may be logical that the spatial-temporal information is provided in case of an event. However, even if the cumulative flow does not change along an observation path, i.e., there is no event, it is still valuable to known the paths along which N is constant.

The observed cumulative flow is a discrete variable. However, to understand the relation of the relative flow to the macroscopic variables flow q, density ρ and mean speed u, we can consider the smoothed and continuously differential cumulative flow. Following (Makigami et al., 1971) the three macroscopic variables can be determined for points in space-time by taking the derivatives to space and time, where $q(x, t) = \partial_t N(x, t)$, $\rho(x, t) = -\partial_x N(x, t)$ and $u(x, t) = q(x, t)/\rho(x, t)$. The smoothed cumulative flow along an observation path is given by $N(X_o(t), t)$, which we denote as $N_o(t)$. This allows us to describe the relative flow along an observation path, which is the derivative to time of the cumulative flow along this path, i.e., $\partial_t N_o(t) = \rho(X_o(t), t)[u(X_o(t), t) - V_o(t)]$.

2.2. Data used in existing studies that estimate in or via the cumulative flow plane

Multiple methodologies have been proposed to estimate the traffic state in the cumulative flow plane. For instance, Newell's (three-detector) method (Newell, 1993a,b,c; Laval et al., 2012), Claudel's method (Claudel and Bayen, 2010a,b) and Sun's method (Sun et al., 2017) can be used to estimate the cumulative flow for points in space-time. Other methodologies have been proposed to estimate traffic flow features that can be directly derived from the cumulative flow curves at link boundaries, e.g., the vehicle accumulation (Van and Hoogendoornn, 2015; Amini et al., 2016) and the travel-time (Bhaskar et al., 2010).

All these studies work with stationary observers that are positioned at the link boundaries. Furthermore, some studies, e.g., Claudel and Bayen (2008, 2010a,b), Bhaskar et al. (2010), Van and Hoogendoornn (2015) and Sun et al. (2017), consider probe trajectory (or vehicle reidentification) data to describe ΔN over a path (the probe trajectory) or between specific points in space-time. Here, it is assumed that the probe vehicles do not overtake other vehicles or are overtaken by other vehicles, i.e., they assume $\Delta N = 0$ over the probe trajectory. The reason for adding the probe trajectory data to the stationary observers is twofold. Firstly, it yields internal conditions (constraints) that can be used in estimation, e.g., Claudel and Bayen (2010a,b). Secondly, intersecting observations paths can be used to initialize the cumulative flow over observation paths and mitigate the cumulative error problem, e.g.,

Bhaskar et al. (2010) and Van and Hoogendoornn (2015).

However, there are important differences between probe trajectory data and relative flow data collected by moving observers. In multi-lane traffic, i.e., if overtaking is possible, the cumulative flow can change over the probe or moving observer trajectory (Sun et al., 2017). This change is not observed by the probes, but is observed by the moving observers. Therefore, moving observers that are part of the traffic flow provide a more accurate representation of the change in cumulative flow over the observation path. Furthermore, depending on the road infrastructure and equipment installed in the vehicle, moving observers can observe the change in cumulative flow for other traffic flows, e.g., opposite traffic flows (Redmill et al., 2011) or parallel traffic flows. For these reasons relative flow data is a good addition and/or alternative to the data considered in Claudel and Bayen (2008, 2010a,b), Bhaskar et al. (2010), Van and Hoogendoornn (2015) and Sun et al. (2017).

3. Model-based traffic state estimation in the cumulative flow plane

This section discusses the principles that can be used for the two processes that are part of a model-based estimation approach, i.e., (1) learning the models that are used in estimation based on historical data and (2) real-time estimation by assimilating real-time data and models, and why the characteristics of relative flow data are valuable for applying these principles. Prior to discussing the two processes, Section 3.1 explains the considered link traffic flow model (L-TFM) and Newell's method (Newell, 1993a,b,c), which is the foundation for the principles introduced in this section. Both processes take part in the cumulative flow plane. For learning the L-TFM, see Section 3.2, this means that we remain in the cumulative flow plane to learn the model parameters. For traffic state estimation, see Section 3.3, this means that we want to estimate $N(x, t)$. Section 3.4 discusses which spatial-temporal data characteristics are desired to apply the principles explained in Sections 3.2 and 3.3.

3.1. Estimation using Newell's method and a triangular fundamental diagram

Newell's method (Newell, 1993a,b,c) can be used to estimate the cumulative flow value for points in space-time. This method requires a LWR-model with a concave and continuous fundamental diagram (FD). For the sake of simplicity, we will illustrate the principles in this paper based on a triangular FD (see Fig. 3a). However, the principles can be extended to other concave and continuous FDs, e.g., piecewise-linear FDs (triangular FD is a two-piece-linear FD), Greenshields FD and Smulders FD. In Section 4, we will apply the principles on data from a stochastic microscopic simulation, where drivers are not bound to a FD, let alone a triangular FD. Hence, Section 4 will also show the accuracy of the results if the assumptions behind the LWR-model with a triangular FD are partially violated.

The conventional LWR-model (Lighthill et al., 1955; Richards, 1956) can be re-written where the cumulative flow is the state variable (Newell, 1993a,b,c):

$$\partial_t N(x, t) - Q(-\partial_x N(x, t)) = 0 \tag{1}$$

where $Q(\cdot)$ is the flow-density FD of traffic flow.

The triangular FD is widely used in traffic state estimation 'because of its simplicity, theoretically preferable features and some empirical evidence' (Seo et al., 2017). This FD can be described by three parameters: free-flow speed v^f, wave speed w and passing rate r, where r describes the relative flow observed by a moving observer that travels at w through any state on the congested branch of the FD. The FD defines the minimum (lower bound) and maximum (upper bound) ΔN between two points in space-time, which are important the variational theory presented by Daganzo (2005). The lower and upper bounds depend on the speed of the line between

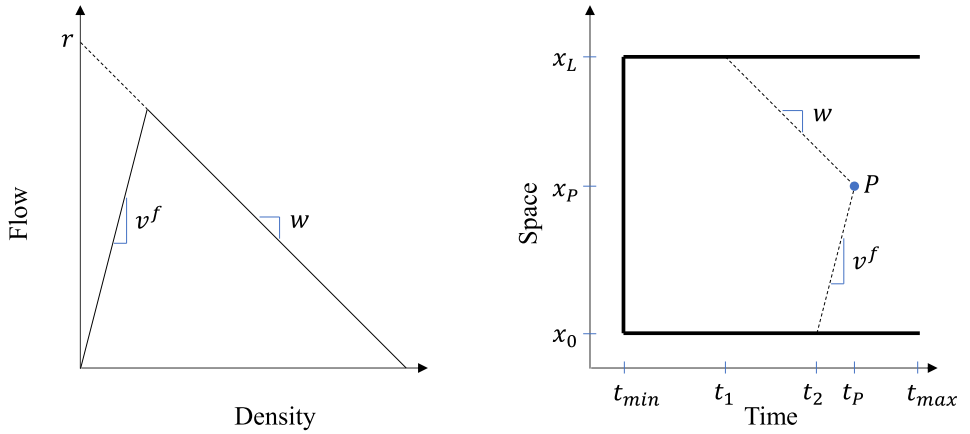

(a) Triangular fundamental diagram with known parameters v^f, w and r.

(b) Estimation of $N(x_P, t_P)$.

Fig. 3. Estimation using Newell's method.

these points. In some studies this line is referred to as a path, e.g., Daganzo (2005); however, to avoid confusion with observation paths, we use the term 'wave'. The triangular FD has two characteristic wave speeds, i.e., v^f and w, which yield two restrictive waves with respectively upper bounds for ΔN of 0 and $r\Delta t$. Following Newell (1993a,b,c), we can estimate the cumulative flow in a point P given a boundary $\mathcal{B}$ over which $N_{\mathcal{B}}$ is known and from which we can draw a v^f-wave and a w-wave to P. In this special situation, the minimum of the two restrictions yields N for P. Fig. 3b provides an example in which N is known for $\mathcal{B}$ (solid black lines) and we want to estimate N for P. The restrictive paths are obtained by drawing lines starting from $\mathcal{B}$ with the characteristics speeds. Next, the cumulative flow for P, i.e., $N(x_P, t_P)$, is estimated using:

$$N(x_P, t_P) = \min[N(x_0, t_2), N(x_L, t_1) + r\cdot(t_P - t_1)] \tag{2}$$

This approach can be followed to estimate $N(x, t)$ for the full space-time domain if we have the initial condition (IC) and boundary conditions (BCs). The IC and BCs describe the cumulative flow curves over the solid black lines that are shown in Fig. 3b i.e., the IC describes $N(x, t_{\min})$ and the upstream and downstream BCs respectively describe $N(x_0, t)$ and $N(x_L, t)$.

3.2. Learning the link traffic flow model

The aim of this section is to explain how relative flow data can be used to learn the link traffic flow model (L-TFM) parameters. For this purpose, we explain how a learning dataset can be constructed using relative flow data that contains combinations of the change in cumulative flow and time over potential characteristic waves, see Section 3.2.1. This part yields fundamental insights that can be used to explain which spatial-temporal (relative) flow data characteristics are valuable to learn the model parameters, see Section 3.4. Next, in Section 3.2.2, we provide the theoretical relations between the Δt- and ΔN-observations over potential characteristics waves and the model parameters.

To learn the L-TFM parameters, an approach is considered for which we remain in the cumulative flow plane. This approach differs from the approaches followed by Dervisoglu et al. (2009), Knoop and Daamen (2017) and Van Erp et al. (2018b), which use flow and density estimates, i.e., $\{q, \rho\}$-estimates, to learn the triangular FD. These approaches fit the free-flow and congested branch in the $\{q, \rho\}$-plane based on the difference between the fitted FD and the $\{q, \rho\}$-estimates. Although this may yield the 'best' fit in the $\{q, \rho\}$-plane, it may not be the most accurate L-TFM for traffic state estimation in the cumulative flow plane.

As explained in the introduction, this study does not design full methodologies as our focus lies on understanding the value of relative flow data. However, the principles explain in this section provide the basis for methodologies that can learn the model parameters based on relative flow data. It is left to future research to design and test such full methodologies and algorithms.

3.2.1. Construct a learning dataset that contains cumulative flow and time over potential characteristic waves

As explained in Section 3.1, a L-TFM can be used to estimate the cumulative flow N for a point P in space-time given that we know N over a boundary $\mathcal{B}$, where all potential restrictive paths can be drawn between $\mathcal{B}$ and P. Following earlier assumptions, we define the model structure of the L-TFM that we want to learn: a LWR-model with a triangular fundamental diagram (FD), see Fig. 3a. In this case, this model has three unknown parameters, i.e., the passing rate r, free-flow speed v^f and wave speed w.

To learn the L-TFM, we want to obtain a learning dataset that describes the change in cumulative flow and time over all potential restrictive waves for points in space-time. Here, all potential restrictive waves are straight lines in space-time that travel with a certain speed, i.e., the potential values of v^f and w. Stationary and moving observers can yield a set of observations paths that allow us to construct a learning dataset that combines ΔN and Δt over potential characteristic waves. If observation paths intersect, the ΔN-observations can be related to each other (Van Erp et al., 2018a). In this way, we can obtain ΔN between two points that lie on the same or different observation paths. Depending on the spatial-temporal characteristics of individual observation paths, we can have a set of intersecting observation paths for which we can draw backwards (in time) propagating waves from a point P that all intersect with an observation path that is part of the set. Fig. 4a and b illustrate two situations in which it is possible to find ΔN and Δt for the potential values of v^c, where v^c is used to describe the speed of a potential characteristic wave. In this figure, we only show a selection of potential values of v^c around v^f and w. However, it is possible to draw waves for other values of v^c.

3.2.2. Learn traffic flow model parameters

This section explains the theoretical relations between the learning dataset, i.e., combinations of ΔN, Δt and v^c, and the L-TFM model parameters. Below, we first explain which values of ΔN and Δt are expected given that the traffic flow follows a known triangular FD. Next, we describe the rate errors, i.e., Υ, over the characteristic waves that are induced by error in the model parameters.

The learning dataset contains the information that is needed to learn the traffic flow model parameters, i.e., v^f, w and r, following Newell's method. For this purpose, Eq. (2) can be rewritten to:

$$0 = \min[\Delta N^{\text{ff}}_{P\mathcal{B}}, \Delta N^{\text{cg}}_{P\mathcal{B}} - r\Delta t^{\text{cg}}_{P\mathcal{B}}] \tag{3}$$

Note that this relation includes the change in cumulative flow and time from P to $\mathcal{B}$. Let us define $\mathcal{B}^{\text{cg}}$ as the point-of-intersection of the w-wave and $\mathcal{B}$, which means that $\Delta N^{\text{cg}}_{P\mathcal{B}} = N(x_{\mathcal{B}^{\text{cg}}}, t_{\mathcal{B}^{\text{cg}}}) - N(x_P, t_P)$ and $\Delta t^{\text{cg}}_{P\mathcal{B}} = t_{\mathcal{B}^{\text{cg}}} - t_P$.

This function can be rewritten to describe the rates that are observed instead of the counts, i.e., $\Delta N/\Delta t$ instead of ΔN:

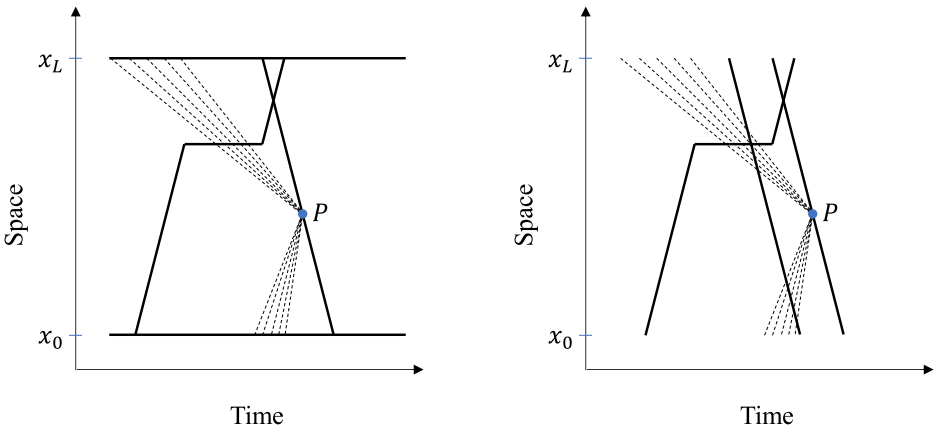

(a) Example that combines stationary and moving observers.

(b) Example that relies on moving observers alone.

Fig. 4. Examples of sets of observation paths (solid lines) that allow us to draw potential backwards (in time) propagating waves from a point P (dashed lines) and obtain combinations of the change in cumulative flow and time over the different waves.

$$0 = \max\left[\frac{\Delta N^{\text{ff}}_{P\mathcal{B}}}{\Delta t^{\text{ff}}_{P\mathcal{B}}}, \frac{\Delta N^{\text{cg}}_{P\mathcal{B}}}{\Delta t^{\text{cg}}_{P\mathcal{B}}} - r\right] \tag{4}$$

In the remainder of this section, we consider the second relation, i.e., Eq. (4). This relation can be interpreted as follows: The cumulative flow in point P is restricted by the v^f-wave, the w-wave or both (at capacity). We use the variable R to describe the restrictive wave, where $R = 1$, $R = 2$ and $R = 3$ respectively denote that the v^f-wave, w-wave or both waves are restrictive. Therefore, for each P the restrictive wave is given by R_P:

$$\begin{aligned}
R_P &= 1 \quad \text{if } \tfrac{\Delta N^{\text{ff}}_{P\mathcal{B}}}{\Delta t^{\text{ff}}_{P\mathcal{B}}} = 0 \text{ and } \tfrac{\Delta N^{\text{cg}}_{P\mathcal{B}}}{\Delta t^{\text{cg}}_{P\mathcal{B}}} - r < 0,\\
R_P &= 2 \quad \text{if } \tfrac{\Delta N^{\text{ff}}_{P\mathcal{B}}}{\Delta t^{\text{ff}}_{P\mathcal{B}}} < 0 \text{ and } \tfrac{\Delta N^{\text{cg}}_{P\mathcal{B}}}{\Delta t^{\text{cg}}_{P\mathcal{B}}} - r = 0,\\
R_P &= 3 \quad \text{if } \tfrac{\Delta N^{\text{ff}}_{P\mathcal{B}}}{\Delta t^{\text{ff}}_{P\mathcal{B}}} = 0 \text{ and } \tfrac{\Delta N^{\text{cg}}_{P\mathcal{B}}}{\Delta t^{\text{cg}}_{P\mathcal{B}}} - r = 0.
\end{aligned} \tag{5}$$

Eq. (4) holds if traffic flow follows a triangular FD and the model parameters are known or correctly estimated. However, without having the correct parameter values, it becomes more challenging to find the restrictive wave.

Let us explore the influence of error in the model parameters on the two elements of Eq. (4), i.e., $\Delta N^{\text{ff}}_{P\mathcal{B}}/\Delta t^{\text{ff}}_{P\mathcal{B}}$ and $\Delta N^{\text{cg}}_{P\mathcal{B}}/\Delta t^{\text{cg}}_{P\mathcal{B}} - r$. In the remainder of this work, $\widehat{v^f}$, $\hat{w}$ and $\hat{r}$ are used to denote the (potentially incorrect) parameter-guesses. Furthermore, ε is used to denote the parameter errors, where the error in v^f is given by $\varepsilon_{v^f} = v^f - \widehat{v^f}$. The observations related to the v^f-wave, i.e., $\Delta N^{\text{ff}}_{P\mathcal{B}}$ and $\Delta t^{\text{ff}}_{P\mathcal{B}}$, are affected by ε_{v^f}, while the observations related to the w-wave, i.e., $\Delta N^{\text{cg}}_{P\mathcal{B}}$ and $\Delta t^{\text{cg}}_{P\mathcal{B}}$, are affected by ε_w. The errors related to the two elements of Eq. (4) are denoted by Υ, where Υ^{cg} describes the error related to $\Delta N^{\text{cg}}_{P\mathcal{B}}/\Delta t^{\text{cg}}_{P\mathcal{B}} - r$. The parameter errors ε_{v^f} and ε_w influence which backwards propagating waves are drawn from point P. The errors Υ^{ff} and Υ^{cg} can be quantified if the mean state through which this wave travels still lies on the restrictive traffic state, e.g., Υ^{cg} can be quantified if the $\hat{w}$-wave still fully travels through congested (including capacity) states:

$$\Upsilon^{\text{ff}} = \varepsilon_{v^f}\bar{\rho} \tag{6}$$

$$\Upsilon^{\text{cg}} = \varepsilon_w\bar{\rho} + \varepsilon_r \tag{7}$$

These equations provide insight in relations between $\Delta N_{P\mathcal{B}}/\Delta t_{P\mathcal{B}}$ for different potential values of the characteristics wave speeds, i.e., $\widehat{v^f}$ and $\hat{w}$. Fig. 5 provides a visual interpretation of the expected relations given that traffic flow follows a triangular FD for points P that are restricted by the w-wave, i.e., the black line (jam state) and the orange line (queue discharge state), and that are restricted by the v^f-wave, i.e., the blue line. The exact shapes of the lines also depend on the non-restrictive traffic conditions and can therefore differ. However, a line related to a point that is restricted by the w-wave should cross (r, w), which is indicated by the red square, and a line related to a point that is restricted by the v^f-wave should cross $(0, v^f)$, which is indicated by the green dot. As every P is restricted by one or both waves, see Eq. (5), every line should intersect with one or both characteristic points, i.e., the red square and/or green dot. Furthermore, if P is not restricted by the characteristic wave related to that characteristic point, it should lie below the characteristic point. As depicted by Eqs. (6) and (7), the slope of the lines depends on the average density. The wave traveling at the wave speed that is restrictive for a point P travels through a single state, e.g., the jam state where $\rho = \rho^j$. Therefore, the slope of the lines in the related characteristic point depends on the density at P. This means that slopes of the black, orange and blue lines will be

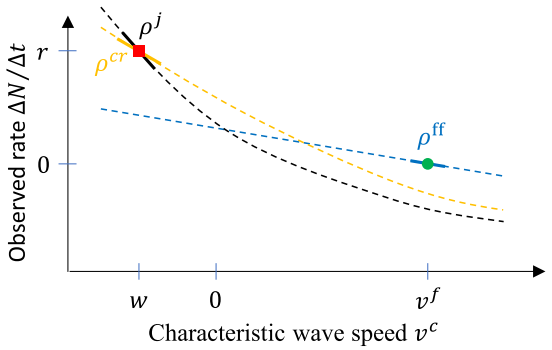

Fig. 5. Expected relations between the observed rates dependent and the considered characteristic wave speed given that traffic flow follows a triangular FD for points that are restricted by the *w*-wave (black and orange lines) and v^f-wave (blue line). (For interpretation of the references to colour in this figure legend, the reader is referred to the web version of this article.)

equal to the jam density ρ^j, the critical density ρ^{cr} and a free-flow density ρ^{ff} at the characteristic point that relates to their restrictive wave. These slopes and densities are indicated in Fig. 5.

3.3. Traffic state estimation using relative flow data and a link traffic flow model

This section explains how relative flow data combined with the L-TFM can be used to (partially) estimate the traffic state for different data availability scenarios. This allows us to evaluate the potential value of relative flow data. The difference in these scenarios lies in the inclusion of stationary observers positioned at the link boundaries.

Fig. 6 shows a data scenario in which all observation paths can be related to each other through intersection. In this scenario, stationary observers positioned at the link boundaries are combined with a set of moving observers. The dots shown in Fig. 6a are used to illustrate the intersection points between the observation paths. The green dots illustrate the initial intersection points of the observers that can be used to define the cumulative flow over all observation paths in one framework. As explained in Van Erp et al. (2018a), this is also a favorable scenario to mitigate the cumulative error problem (CEP), which is also referred to as the cumulative drift problem (Van and Hoogendoornn, 2015), due to the intersection of already initialized observation paths (indicated by the blue dots in Fig. 6a). As all observation paths are connected, Newell's method can be applied to estimate the cumulative flow for points that do not lie on an observation path. The space-time domain for which $N(x, t)$ can be estimated using this method is indicated with a grey area in Fig. 6b.

In the remainder of this section, we will consider a more restrictive data scenario that solely includes moving observers. Compared to the data configuration shown in Fig. 6, no stationary observers are positioned at the link boundaries. By removing the stationary observers at the link boundaries, the observation paths are no longer connected at these boundaries and there are no observation paths that fully cover the link boundaries. As a result, the boundary conditions (BCs) are not obtained and the remaining observation paths can be (partially) unconnected.

However, by combining these observation paths with information in the form of traffic flow models, we may obtain information

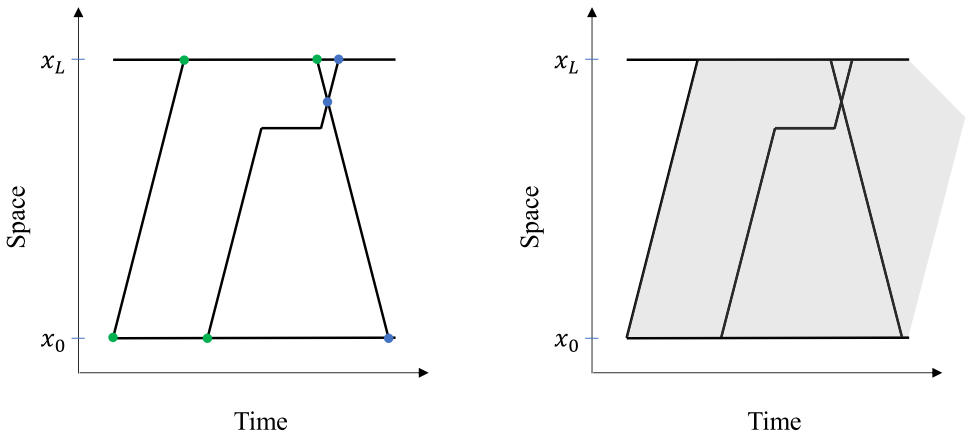

(a) Observation paths and intersection points.

(b) Space-time domain for which $N(x, t)$ can be estimated using Newell's method.

Fig. 6. Data scenario that combines stationary observers positioned at the link boundaries and a set of moving observers.

on the link BCs and connect observation paths. The principles that can be used for this purpose are discussed below. First, Section 3.3.1 discusses which information remains without the availability of stationary observers on an individual link. Next, we explain why it is beneficial to estimate the traffic state in a network of links and nodes, where information can propagate over a node, i.e., from link to link (Section 3.3.2).

The principles explained below can be used to design a full methodology that assimilates relative flow data and the traffic flow model to estimate the traffic state on a single or set of links. Such a to-be-developed full methodology should be able to exploit the valuable interactions of information (i.e., data and models) in space-time and thereby estimate 'the most probable state'. For this purpose, different assimilation techniques can be considered (Seo et al., 2017).

3.3.1. *Information propagation on an individual link when relying on moving observers only*

This section explains how relative flow data and the link traffic flow model (L-TFM) can be combined to connect observation paths and estimate the BCs. Furthermore, we explain how the demand D (downstream boundary) and supply S (upstream boundary) can be estimated, which are valuable for information propagation in a network, see Section 3.3.2. To explain which information is available on an individual link, we often refer to Fig. 7. This figure shows the observation paths of four moving observers (solid black lines) that are numbered at the point they enter the link in Fig. 7a. Again, a LWR-model with a known triangular FD is considered.

Intersecting observation paths can form sets that allow us to describe the relation in ΔN between certain points on the link boundaries (see Fig. 7b). A moving observer that crossed both boundaries describes $N(x_0,\, T_m(x_0)) - N(x_L,\, T_m(x_L))$, where $T_m(x_0)$ and $T_m(x_L)$ respectively denote the times at which moving observer m crossed the upstream and downstream link boundary. Furthermore, if observation paths intersect, more points on the boundaries can be related to each other. Out of the four observation paths shown in Fig. 7b only those of moving observers m_2 and m_3 intersect. The cumulative flow over these paths can thus be related to each other based on their intersection point.

From one set of connected observation paths, using Newell's method we may be able to estimate N for points that lie observation paths that are not connected via intersection (see Fig. 7c). For instance, for the case shown in Fig. 7c, we can estimate $N(x_P,\, t_P)$ in the N-framework used for moving observers m_2 and m_3. As point P lies on the observation path of moving observer m_4, the cumulative flow over that observation path can be described in the same framework. However, we still miss information to describe the observation path of moving observer m_1 in the same framework. With this information the link outflow between $T_{m_1}(x_L)$ and $T_{m_2}(x_L)$ and link inflow between $T_{m_1}(x_0)$ and $T_{m_3}(x_0)$ remain unknown. However, the two unknowns are related, i.e., if information related to $N(x_L,\, T_{m_2}(x_L)) - N(x_L,\, T_{m_1}(x_L))$ is obtained we can describe $N(x_0,\, T_{m_3}(x_0)) - N(x_0,\, T_{m_1}(x_0))$.

In the case of a triangular FD (as is assumed here), Newell's method relies on two forward (in time) propagating waves, i.e., one traveling at free-flow speed v^f and one traveling at wave speed w. The FD describes the maximum change in N as a function of time over these waves, i.e., 0 for the v^f-wave and $r\Delta t$ for the w-wave. Combined with the knowledge that one of these two upper bounds is restrictive, we can estimate N for the point where these two waves intersect. Newell's method (in this form) cannot be used to estimate N for a point in space-time on the link boundary as only one of the two time-forward propagating waves intersects with the link boundary, i.e., v^f-wave and w-wave respectively intersect with the downstream and upstream boundary. However, the individual waves do yield restrictions on ΔN, where forward and backward (in time) propagating waves respectively yield an upper and lower bound for ΔN. Fig. 7d shows a point (grey dot) in space-time together with two backwards (blue dashed arrow lines) and forward (red dashed arrow lines) propagating waves. Given that we know N for the point indicated by the grey dot, the waves provide upper and lower bounds for points on the link boundaries. We focus on these four paths as they play an important role in the remainder of this section. However, we can find upper and lower bounds for ΔN for any two points in space–time. Therefore, if we have a set of observation paths for which N is initialized (i.e., N is defined in the same framework for all paths that are part of the set), we can use all point that lie on these observation paths to find upper and lower bounds for $N(x_0,\, t)$ and $N(x_L,\, t)$.

By exposing the restrictive wave we can (partially) estimate the boundary conditions. As stated above, we cannot reach a point on the link boundaries with a forward propagating v^f-wave and w-wave that start from a point on the link. However, in some cases, we can find that a forward propagating wave originating from the boundary is restrictive. The forward propagating waves from the upstream and downstream boundaries are respectively the v^f-wave and w-wave. A forward propagating wave starting from a point on the link boundary (with unknown N) can intersect with the other forward propagating wave starting from a point and in a point for which N is known. If the forward propagating wave between the two points with known N is not restrictive, the forward propagating wave from the link boundary has to be restrictive. This information allows us to estimate N at the link boundaries. To explain this we consider the examples shown in Fig. 7e and f, which respectively relate to estimating N for a point on the downstream and upstream boundary. In these figures the two black dots indicate points in space-time for which we known ΔN (as they both lie on a set of connected observation paths). If this wave (indicated by the red dashed arrow line) is not restrictive, i.e., $\Delta N < 0$ for Fig. 7e and $\Delta N < r\Delta t$ for Fig. 7f, the wave from the link boundary has to be restrictive. Therefore, we can use a backwards propagating wave to the link boundary (indicated by the blue dashed arrow line) to estimate N on the link boundary.

Supply S and demand D can be partially estimated based on the BC estimates and direct upper bound restrictions of the boundary conditions (see Fig. 7g and h). Direct upper bound restrictions are obtained using by drawing forward propagation waves with the speeds v^f and w, i.e., the red dashed arrow lines in Fig. 7d, from points on the observation paths to the link boundaries. We use the notations $\widetilde{N}^+(x_0,\, t)$ and $\widetilde{N}^+(x_L,\, t)$ are used for these upper bound restrictions, which are respectively obtained using w-waves and v^f-waves. Demand and supply depend on the density at the link boundaries, see Fig. 8a and b. The critical density ρ^{cr} plays an important role in estimating D and S. As can be seen in Fig. 8a and b, D and S are respectively equal to the capacity q^C in over-critical ($\rho \geqslant \rho^{cr}$) and under-critical ($\rho \leqslant \rho^{cr}$) densities. Furthermore, D and S are respectively described by the free-flow and congested FD branch in under-critical ($\rho \leqslant \rho^{cr}$) and over-critical ($\rho \geqslant \rho^{cr}$) densities. We include $\rho = \rho^{cr}$ both in under- and over-critical densities as

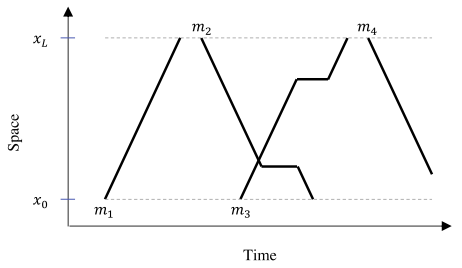

(a) Space-time diagram showing the observation paths of four moving observers (solid black lines).

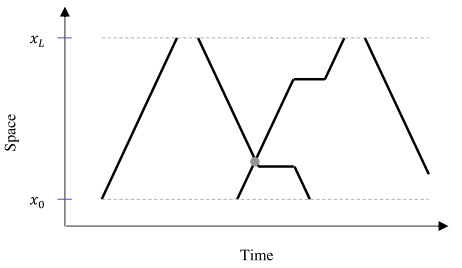

(b) Connecting observation paths via intersection.

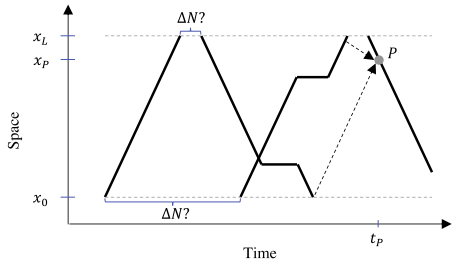

(c) Connecting observation paths via L-TFM estimates.

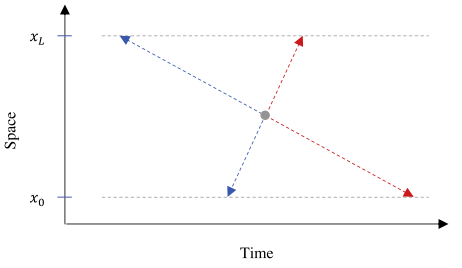

(d) Restrictive paths from a point in space-time to the link boundaries.

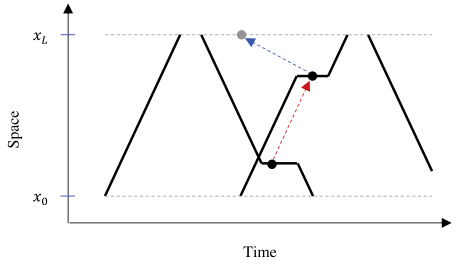

(e) Estimate grey point on $N(x_L, t)$.

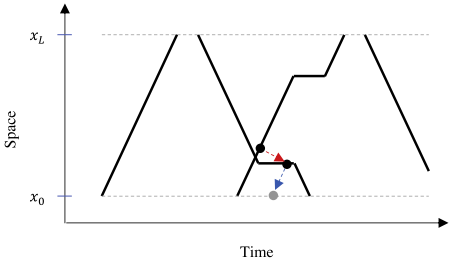

(f) Estimate grey point on $N(x_0, t)$.

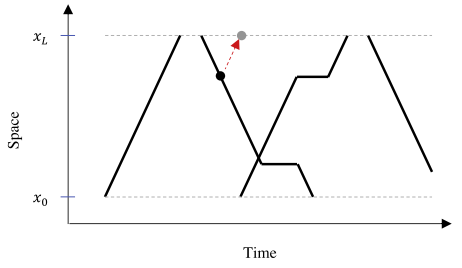

(g) Find direct upper restriction for grey point on $\tilde{N}^+(x_L, t)$.

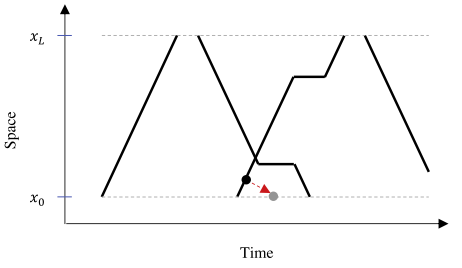

(h) Find direct upper restriction for grey point on $\tilde{N}^+(x_0, t)$.

Fig. 7. Example of information that is available on an individual link.

D and S are equal to q^C and are correctly described by the FD branches in this point. By comparing the link BC estimates and direct upper bound restrictions, we can find whether the density at the link boundary is under-critical or over-critical. For the upstream boundary, $\tilde{N}^+(x_0, t) > N(x_0, t)$ and $\tilde{N}^+(x_0, t) = N(x_0, t)$ respectively describe under-critical and over-critical densities. For the upstream boundary, $\tilde{N}^+(x_L, t) > N(x_L, t)$ and $\tilde{N}^+(x_L, t) = N(x_L, t)$ respectively describe over-critical and under-critical densities. For the cases in which the link boundary condition estimates and direct upper bound restrictions are equal, D and S are equal to respectively the outflow and inflow, i.e., $\partial_t N(x_L, t)$ and $\partial_t N(x_0, t)$.

In some cases, we may not be able to determine the boundary conditions, while we can determine whether the link boundary density is under- or over-critical. If we known that the upstream and downstream boundary densities are respectively under-critical and over-critical, we known that supply and demand are equal to the capacity q^C. As an example, we consider a moving observer that

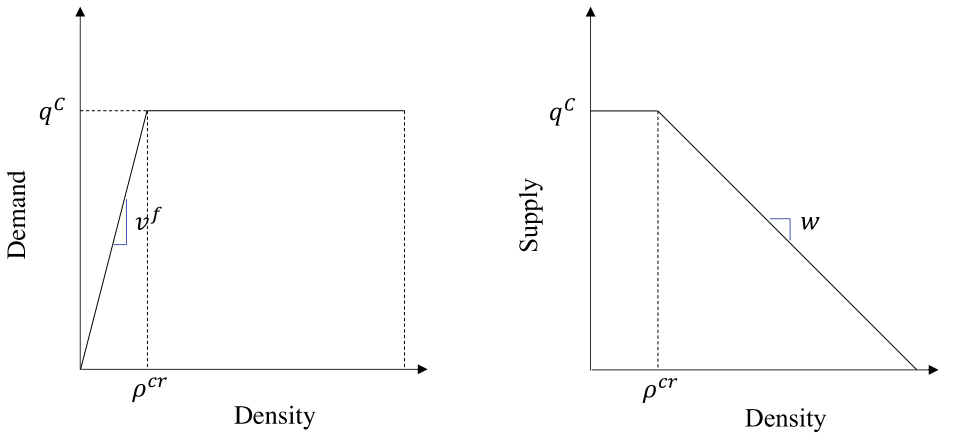

(a) Demand as a function of density at the downstream link boundary.

(b) Supply as a function of density at the upstream link boundary.

Fig. 8. Demand and supply curves.

travels in the opposing flow direction with free-flow speed. Starting on this observation path, we can draw forward propagating v^f-waves and w-waves that allow us to estimate ΔN with respect to the observation path for an area in space–time. If a v^f-wave is not the restrictive wave for at least one point that it crosses, $D = q^C$ at the intersection of this v^f-wave and the downstream boundary. Similarly, if a w-wave is not the restrictive wave for at least one point that it crosses, $S = q^C$ at the intersection of this w-wave and the upstream boundary.

The techniques discussed in this section allow us to partially determine the boundary conditions, demand and supply, based on the information that is available on an individual link. Below, we explain why it is beneficial to use information that is available in a network of links and nodes to estimate the traffic state. Furthermore, we explain why the link boundary estimates from one link can help to estimate the boundary conditions on an other, connected link.

3.3.2. Information within a network of links and nodes

As explained above, the information available on individual links may yield estimates of the link inflow, outflow, demand and supply. However, the moving observers combined with the L-TFM may not provide sufficient information to estimate the full link boundary conditions. To overcome this problem, it is valuable to add information that is available for other parts of the road network.

The road network can be represented using links and nodes, where the nodes connect multiple in-flowing and out-flowing links. There are many different types of nodes in the road traffic network, e.g., inhomogeneous nodes, merge nodes, diverge nodes, cross nodes (Yperman, 2007). In general, motorway intersection nodes are less complex than urban intersection nodes. For instance, motorway nodes will often connect less links and there is no turn delay. The latter means that a vehicle that exits an in-flowing link will instantaneously enter an out-flowing link.

The conservation-of-vehicles condition can be used for information propagation over nodes. Especially, for simple nodes (e.g., those that are used to describe a lane drop, on-ramp or off-ramp) this condition can suffice to (partially) estimate the flow over the node and in this way estimate the link boundary conditions from the node. For instance, in case of a lane drop (i.e., an inhomogeneous node), we may be able to estimate the outflow of the in-flowing link during a period, while this is not possible for the inflow of the out-flowing link. By applying the conservation-of-vehicles conditions, the inflow of the out-flowing link can be estimated.

However, additional information may be added in the form of node traffic flow models (N-TFMs), which can be used to describe the traffic behavior over a node. These models can describe the flow over a node as a function of the demand and supply. As explained in Section 3.3.1, relative flow data combined with a L-TFM can provide (partial) estimates for the link boundary conditions, i.e., $N(x_0, t)$ and $N(x_L, t)$. Furthermore, the demand D (which relates to the downstream link boundary) and supply S (which relates to the upstream link boundary) can be (partially) estimated. Partial information (i.e., if we are able to estimate a part of the flows, demands and supplies) in combination with a N-TFM may suffice to estimate the other variables (i.e., the flows, demands and/or supplies that we could not estimate on the individual links). Furthermore, for some periods we may be able to estimate all variables (potentially by involving the conservation-of-vehicles conditions). This yields a learning dataset that combines the dependent and explanatory variables of a N-TFM, which therefore may be used to learn the N-TFM.

Learning N-TFMs and estimating the traffic state in a network of links and nodes is left for future research. It is important to understand that estimation in a network can be valuable to overcome the limitation of not observing the link boundaries using stationary observers, and that estimates from individual links provide the information valuable to apply and learn N-TFMs.

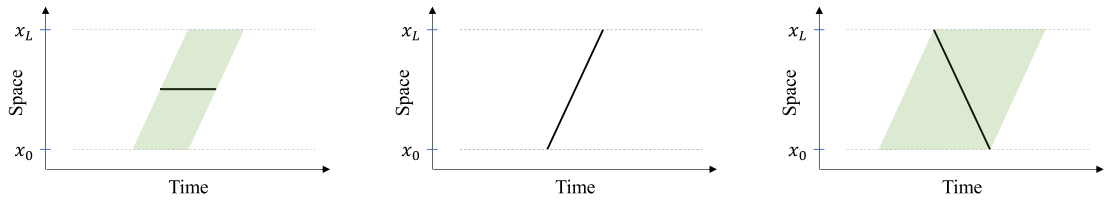

(a) Observer speed = 0 m/s, v^f-wave. (b) Observer speed = v^f m/s, v^f-wave. (c) Observer speed = $-v^f$ m/s, v^f-wave.

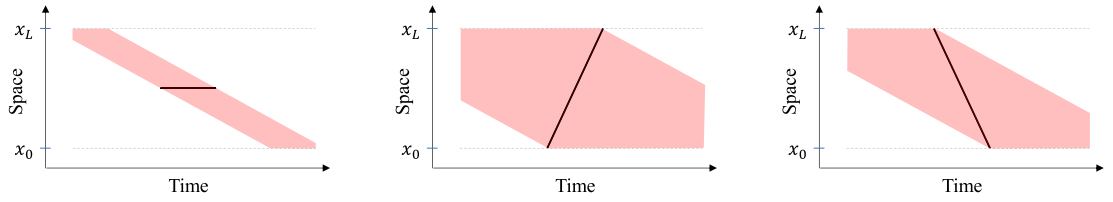

(d) Observer speed = 0 m/s, w-wave. (e) Observer speed = v^f m/s, w-wave. (f) Observer speed = $-v^f$ m/s, w-wave.

Fig. 9. Visualization of the spatial-temporal area for which forward or backwards propagating characteristic waves can be drawn.

3.4. Desirable spatial-temporal data characteristics

The spatial-temporal characteristics of the relative flow data affect the intersections of observation paths and the space–time areas for which it is possible to draw forward or backwards propagating characteristics waves from the observation paths. Both play an important role in the two processes that were discussed in Sections 3.2 and 3.3.

Observation paths only intersect if they have different speeds. A set of moving observers that travel at the same speed or a set of stationary observers (which all travel at 0 m/s) will not intersect. Therefore, combining stationary observers with moving observers or moving observers that observe both their own and opposite travel direction is beneficial to learn traffic flow models.

Furthermore, the area in space-time for which it is possible to draw forward or backwards propagating characteristics waves depends on the observer speed, see Fig. 9. In this figure, we consider three observers that travel at 0, v^f and $-v^f$ m/s, and which collect relative flow data for the same time period. These three observers illustrate a stationary observer (or moving observer at standstill), and moving observers traveling freely in the direction of interest and in opposite direction. The figures show that an increase in the absolute difference between the observer and characteristics wave speeds yields an increase in the spatial-temporal area for which the characteristic wave can be drawn.

For a certain set of observers it may be possible to (partially) estimate the traffic state while it does not provide observations for the learning dataset. The link traffic flow model can be learned based on historical data. This means that we can rely on relative flow data that is collected over a longer period, e.g., months or years. Therefore, is does not have to be a problem that real-time data provide insufficient observations to learn the link traffic flow model.

To obtain observations for the link traffic flow model learning dataset, we need to be able to draw both backwards (in time) propagating waves for the potential values of the characteristic wave speeds between points that lie on observation paths that are connected through intersection. In estimating the traffic state, we work with a single value instead of a potential range for the characteristic wave speeds. Furthermore, each principle presented in Section 3.3.1 puts less requirements on the data than obtaining observations for the learning dataset does: (1) To connect observation paths using Newell's method, we need to draw both backwards moving characteristic waves from a point P to points that lie on the same or connected observation paths, but do not have to be connected to the observation path of point P. (2) To judge whether a characteristic wave is not restrictive for a point on an observation path (which is the basis for estimating the boundary conditions), we need to draw one backwards moving characteristic wave to a point on a connected observation path. And, (3) To estimate supply and demand, we need to draw one forward propagating characteristic wave to points on the link boundary conditions or intermediate points that can be estimated.

4. Testing the principles using simulated data

In this section, the principles explained in Sections 3.2 and 3.3 are tested on simulated data that is collected using the microscopic simulation program VISSIM, which is empirically validated (Fellendorf and Vortisch, 2001). Fig. 10a shows the road network for which traffic is simulated. To test the principles, we consider a single one-lane link, which is highlighted with a white arrow in Fig. 10a. The outflow of this link is constricted by a traffic light, which causes queues to build up on the link. Fig. 10b shows the trajectories on the considered link during the 1800 s simulation period.

Different examples are considered to understand and to test the principles and thereby show how relative flow data can be used in model-based estimation. In these examples, it is assumed that a set of moving observers, which are part of the observed link and opposing link, collect disaggregated relative flow data. It is thus assumed that all individual passings are observed by the moving

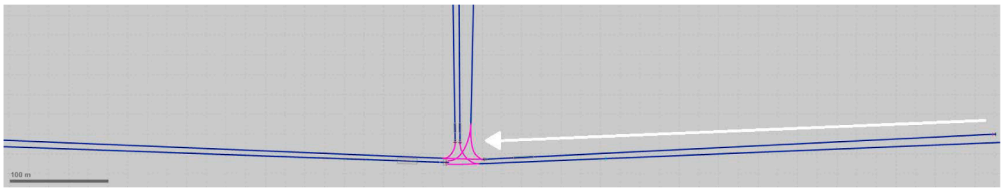

(a) Road network for which traffic is simulated.

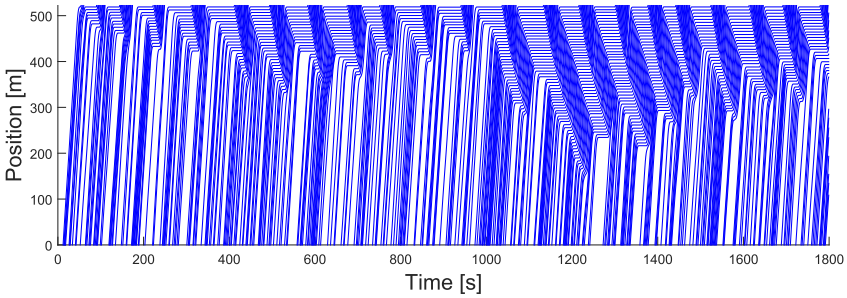

(b) Vehicle trajectories during the 1800 s simulation period.

Fig. 10. VISSIM road network and simulated vehicle trajectories.

observers, which allows us to find the change in cumulative flow between any two points that lie on the same or different intersecting observation paths.

The principles used to extract the valuable information from the relative flow data depend on the process, i.e., learning the link traffic flow model parameters (see Section 4.1) or estimating the traffic state (see Section 4.2). Therefore, each section starts with an explanation of the steps that will be taken in that section.

4.1. Learning the link traffic flow model parameters

To learn the link traffic flow model parameters the following steps are taken: (1) Define the points P. (2) Define the potential characteristics wave speeds and draw the backwards propagating potential characteristic waves. (3) Determine $\Delta N_{P\mathcal{B}}$ and $\Delta t_{P\mathcal{B}}$ for each combination of P and potential characteristics wave speeds. (4) Visualize and interpret the observed rates, i.e., $\Delta N_{P\mathcal{B}}/\Delta t_{P\mathcal{B}}$. And, (5) Approximate the model parameters free-flow speed v^f, wave speed w and passing rate r. In the last step, we approximate the model parameters based on the considered examples. These approximated model parameters will be used to estimate the traffic state in Section 4.2.

Fig. 11(a–d) show space-time plots in which the moving observer observation paths (thick black lines) and other vehicle trajectories (thin blue lines) are visualized. Six points P that lie on an observation path of a moving observer traveling on the opposing road are considered, which are indicated with six different shapes and colors. From the trajectory plots, we know that the restrictive wave for the green square and the cyan hexagram (see Fig. 11a and d) is the v^f-wave, while the others (see Fig. 11b, c and d) are restricted by the w-wave.

Backwards traveling potential v^f-waves and w-waves can be drawn that originate from the points P. In our example, seven potential values are considered for both characteristic waves. The potential values selected for the $\widehat{v^f}$-wave are 13.0, 13.5, 14.0, 14.5, 15.0, 15.5 and 16.0 m/s and the potential values selected for the $\widehat{w}$-wave are -3.0, -3.5, -4.0, -4.5, -5.0, -5.5 and -6.0 m/s. These are visualized in Fig. 11(a–d) using green ($\widehat{v^f}$-wave) and red ($\widehat{w}$-wave) lines.

In these examples, all potential characteristic waves intersect with the observation paths of connected moving observers, which allows us to determine $\Delta N_{P\mathcal{B}}$ and $\Delta t_{P\mathcal{B}}$ for each wave. Fig. 11e and f show the observed rates, i.e., $\Delta N_{P\mathcal{B}}/\Delta t_{P\mathcal{B}}$, for the potential characteristic wave speeds. Here, the shape and color describes the point P that relates to the $\Delta N_{P\mathcal{B}}/\Delta t_{P\mathcal{B}}$-observation.

The figures provide three main insights: (1) The restrictive characteristic wave is clear for each point. The points for which the v^f-wave is restrictive, i.e., the green square and the cyan hexagram, show near-zero values of $\Delta N_{P\mathcal{B}}/\Delta t_{P\mathcal{B}}$ in Fig. 11e, while the rates of the potential v^f-waves for the other points show clear negative values. In Fig. 11f the smallest $\Delta N_{P\mathcal{B}}/\Delta t_{P\mathcal{B}}$-value is observed for the points for which the v^f-wave is restrictive. (2) The spread in the rates observed by the different potential characteristic wave speeds is proportional to the density. For instance, the spread in the rates related to the considered $\widehat{w}$-wave speeds is larger for waves that travel through jam density (i.e., the black diamond and the yellow circle) than for those that travel through a queue discharge state (i.e., the blue triangle and the red pentagram), see Fig. 11f. (3) There seem to be two different queue discharge states, which occur dependent on whether or not vehicles are able to exit the link within that green period. This difference can be observed in Fig. 11f, where the $\Delta N_{P\mathcal{B}}/\Delta t_{P\mathcal{B}}$-value indicated by the red pentagram are higher than those indicated by the blue triangle. When comparing the space–time plots related to these points, we observe that the waves related to the red pentagram cross the trajectories of vehicle that

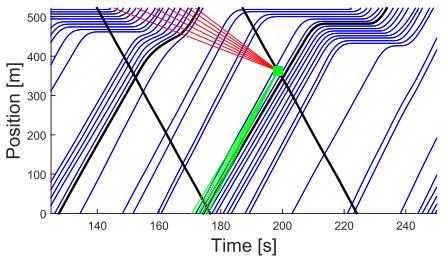

(a) Space-time plot with green square.

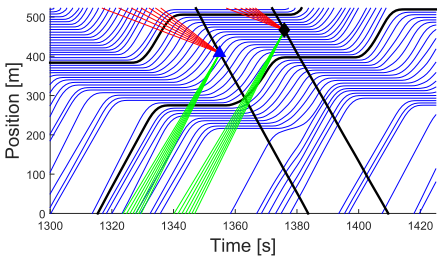

(b) Space-time plot with blue triangle and black diamond.

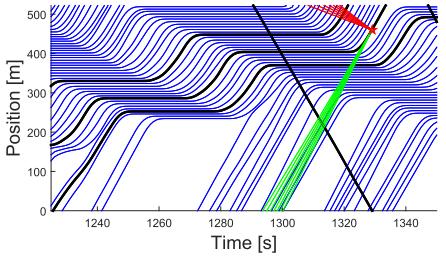

(c) Space-time plot with red pentagram.

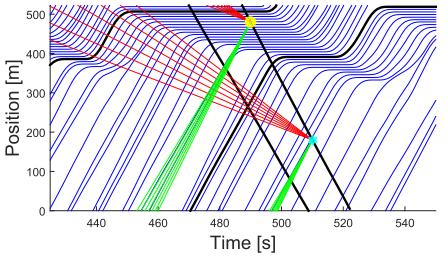

(d) Space-time plot with yellow circle and cyan hexagram.

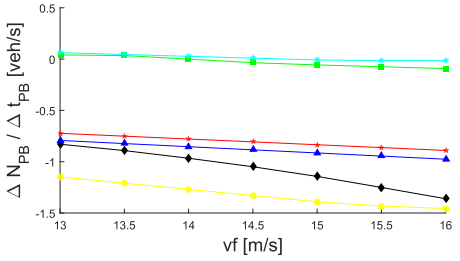

(e) Plot of observed rates and potential values selected for the $\hat{v^f}$-wave.

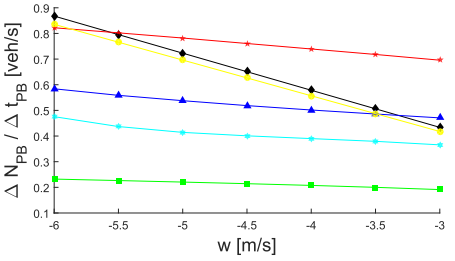

(f) Plot of observed rates and potential values selected for the $\hat{w}$-wave.

Fig. 11. Examples that are considered to learn the link traffic flow model parameters.

exit the link in that green period. These plots also show that these vehicles have a smaller headway than the vehicles that need to wait at least one more red period. It seems that the vehicles 'anticipate' that they will not be able to catch the green light and therefore accelerate slower.

The first two insights are in line with the principles explained in Section 3; however, the third insight indicates that Newell's method in combination with a triangular FD will not yield perfect estimates. As explained in Section 3.2.2: If all points that are restricted by the *w*-wave would lie on the congested branch of a triangular FD, the lines related these points would all intersect in the same point in Fig. 11f. In the $(\Delta N_{P\mathcal{B}}/\Delta t_{P\mathcal{B}}, \hat{w})$-plane this intersection point would lie at (r, w). Instead, we approximate two intersection points in Fig. 11f, i.e., (0.815 veh/s,-5.70 m/s) and (0.485 veh/s, −3.40 m/s), which respectively include the queue discharge states related to vehicles that exit the link within that green period and related to the vehicles that have to wait at least one more red period. Therefore, we will respectively refer to these parameter sets as 'queue-to-queue congested wave parameters' and 'link outflow congested wave parameters'. In Section 4.2 both combinations of $\hat{w}$ and $\hat{r}$ will be used to estimate the traffic state. This allows us to discuss the effect on the estimation accuracy of selecting one of the two combination. Furthermore, for traffic state estimation, we need to define the free-flow speed. Therefore, based on Fig. 11e, $\hat{v^f}$ is set to 14.5 m/s because the $\Delta N_{P\mathcal{B}}/\Delta t_{P\mathcal{B}}$ for the green square and cyan hexagram are closest to zero for this value.

4.2. Estimating the boundary conditions based on moving observers alone

The principles explained in Section 3.3 are applied to estimate the traffic state. In this case study, the focus lies on partially estimating the link boundary conditions based on moving observers alone. For this purpose the following two steps are taken: (1) finding the restrictive wave for points along the observation paths and (2) estimating the link boundary conditions, i.e., $N(x_0, t)$ and $N(x_L, t)$. Fig. 12a shows the example case that is considered in this section. Again, the moving observers and the other vehicle trajectories are respectively plotted with thick black and thin blue lines. In this case, all observation paths can be related to each other through intersection.

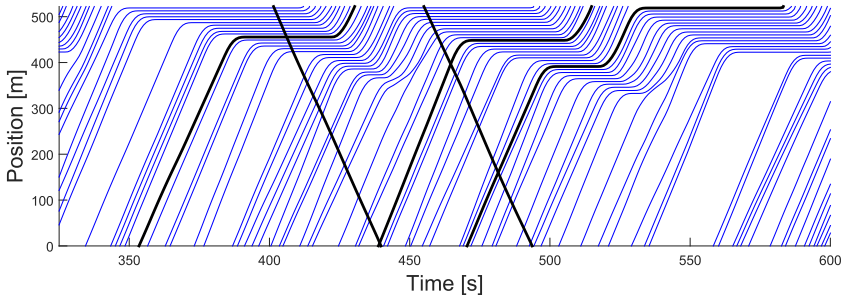

(a) Trajectories and moving observers.

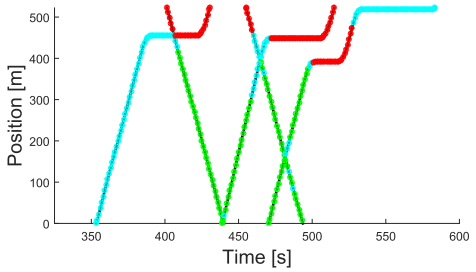

(b) Restrictive waves that are found by excluding the other characteristic wave (queue-to-queue congested wave parameters).

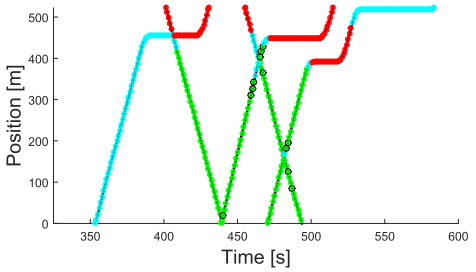

(c) Restrictive waves that are found by excluding the other characteristic wave (link outflow congested wave parameters).

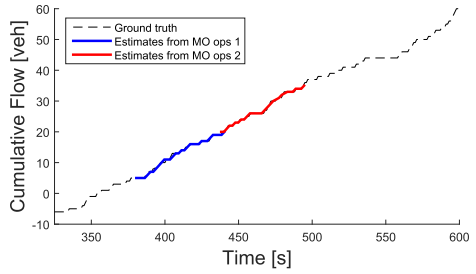

(d) True and partially estimated link inflow cumulative curves (queue-to-queue congested wave parameters).

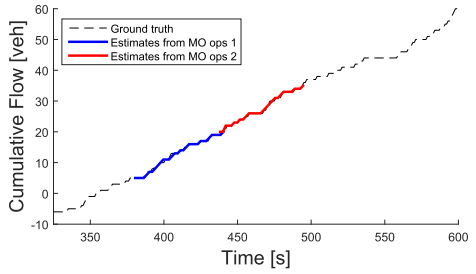

(e) True and partially estimated link inflow cumulative curves (link outflow congested wave parameters).

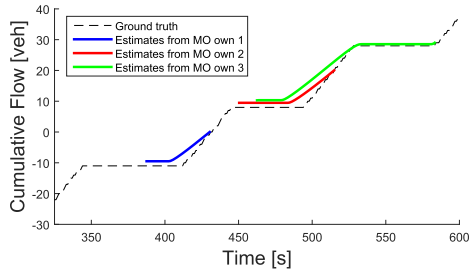

(f) True and partially estimated link outflow cumulative curves (queue-to-queue congested wave parameters).

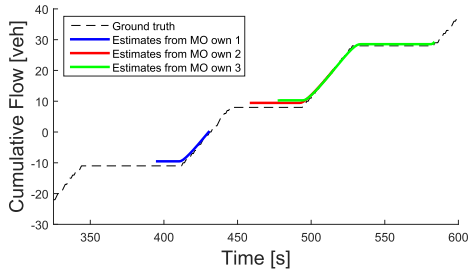

(g) True and partially estimated link outflow cumulative curves (link outflow congested wave parameters).

Fig. 12. Explanation of principles that can be used to estimate the traffic state.

The restrictive wave for points along the observation paths are found by excluding that the other wave is restrictive. For this purpose, characteristics waves are drawn between points of connected observation paths. Given that the change in cumulative flow and time are known for waves drawn between points of connected observation paths, it is possible to judge whether these waves are not restrictive for the point furthest in time. As traffic behavior has a stochastic component, we use a threshold value to judge whether a wave is not restrictive. A v^f-wave and w-wave are respectively said to be non-restrictive if $\Delta N^{\text{ff}}_{P\mathcal{B}}/\Delta t^{\text{ff}}_{P\mathcal{B}} < -0.05$ veh/s and

$\Delta N^{cg}_{P\mathcal{B}}/\Delta t^{cg}_{P\mathcal{B}} - \hat{r} < -0.05$ veh/s. In these cases, the other backwards propagating wave is said to be restrictive. Fig. 12b and c show the results of this approach for the two different parameter sets that we found in Section 4.1. In these figures, the colors green, red and cyan respectively denote that the v^f-wave is restrictive, the w-wave is restrictive or that the restrictive wave is not found. The differences in $\hat{w}$ and $\hat{r}$ cause a few differences in the points for which the v^f-wave is found to be restrictive. These points are indicated using a black circle in Fig. 12c.

To estimate the upstream and downstream boundary conditions, i.e., $N(x_0, t)$ and $N(x_L, t)$, we respectively draw backwards propagating v^f-waves and w-waves origination from the points on the observation paths for which these waves were found to be restrictive. The estimated change in cumulative flow over these waves depends on the characteristic wave, i.e., $\Delta N^{ff} = 0$ veh and $\Delta N^{cg} = -\hat{r}\,\Delta t^{cg}$ veh. An additional assumption that follows from the assumed traffic flow model is used in estimation. After a vehicle that is part of the observed flow is initially restricted by the w-wave, it remains restricted by this wave for the remaining time it is on the link. Again, we consider the two model parameter sets. This yields four figures that depict the estimated (upstream or downstream) boundary conditions related to one of the parameter sets, see Fig. 12(d–g). The figures show the true cumulative curves together with the estimates related to the observation paths of individual moving observers that travel in opposite direction than the related characteristic wave. For instance, for the upstream boundary (which relates to the v^f-wave) the moving observers (MOs) that travel with a negative speed in space–time are shown. In all figures the cumulative flow is set to zero for the point in space–time at which the first moving observer enters the link, i.e., $N(x_0, 354) = 0$.

Fig. 12d and e show that the upstream boundary conditions are accurately estimated for the periods that information is available. These figures are equal as both parameter sets use the same $\widehat{v^f}$ and in both cases the observation paths are found to be restricted by the v^f-wave starting from the same time instances. Fig. 12f and g show a larger difference between the estimates related to the two model parameters sets. The downstream boundary conditions are more accurately estimated for the second set, see Fig. 12g. In Fig. 12f, both the $\hat{w}$ and $\hat{r}$ seem to contribute to the errors in found in the boundary condition estimates. As a result, the slope during the green periods (link outflow) and the shockwave-speed (which according to kinematic wave theory should be w in this case) are respectively underestimated and overestimated (i.e., $\hat{w}$ should have a larger negative value). The overestimation of $\hat{w}$ leads to an earlier estimated start of the green period. Although the model parameters set used in Fig. 12g lead to more accurate estimates of the link outflow cumulative curves, it seems that $\hat{w}$ is underestimated. This may be caused by stochasticity in the traffic behavior in combination with the fact that we only used a limited set of observations to approximate the model parameters.

The case study presented in this section shows that relative flow data collected with moving observers provides information that is valuable to learn the traffic flow model parameters and estimate the unobserved boundary conditions. Furthermore, we observe that the traffic flow simulated using VISSIM has two different queue outflow states, i.e., one related to vehicles that are able to leave the link within this green period and one related to vehicles that have to wait at least one more red period. Therefore, the assumptions behind the LWR-model with triangular FD are partially violated, which negatively influences the estimation accuracy. The voilation of the model assumptions was exposed using relative flow data, see Fig. 11e and f. We may use the same learning dataset to expose which traffic phenomena occur and find the model that best describes traffic flow behavior. As stated in Section 3.1, the principles explained in this paper may be extended the LWR-model with other concave and continuous fundamental diagrams since this still allows us to apply Newell's method. However, the anticipation-behavior exposed in this simulation cannot be captured by the first-order LWR-model. This anticipation-behavior is included in second-order models such as the PW-model. Traffic behavior captured by such higher-order traffic flow models may still be captured in the cumulative flow plane using relative flow data. Further research into this topic is beyond the scope of the current paper.

5. Conclusions and insights

This paper presents the value of relative flow data in estimating the cumulative flow in space-time. To present the value of data, we take the perspective of a model-based estimation approach. In model-based estimation two processes are important: (1) information assimilation (IA) of real-time data and models and (2) learning models that are used in IA based on historical data. This study shows how relative flow data can be used for both processes and why the data characteristics (i.e., the observed variable in combination with the spatial-temporal characteristics) are valuable in traffic state estimation.

This study shows that relative flow data can be used to learn the link traffic flow model and to estimate the traffic state in the cumulative flow plane. If traffic flow follows the LWR-model with a triangular fundamental diagram (FD), relative flow data can be used to find the model parameters. Furthermore, relative flow data can be used to expose that the assumptions behind the LWR-model with a triangular FD are violated. The case study showed that these model assumptions were partially violated for the simulated (using VISSIM) traffic. Furthermore, this study explains that to estimate the traffic state, it is valuable to rely on a combination of moving observers and stationary observers positioned at the link boundaries. However, it also presents principles that can be used to relate the observation paths to each other, estimate the boundary conditions, and estimate the link supply and demand, for the scenario in which we rely on moving observers alone. The simulation study shows that it is possible to partially estimate the link boundary conditions using relative flow data that is collected by moving observers alone. The accuracy of these boundary conditions estimates depends on the ability to learn the model parameters that best describe the traffic flow behavior.

The principles explained in this study yield insights for the valuable characteristics of the relative flow data in model-based traffic state estimation. The valuable characteristics are: (1) Relative flow data provide information on the change in cumulative flow over paths in space-time. For this purpose the observer needs to observe all passings (overtakings), which means that all lanes should be observed, i.e., the full width of the road lie in the sensors range. (2) The observers that collect relative flow data should travel at

different speeds through space and time. This is valuable as the observation paths of observers that travel at different speeds can intersect, which allows us to relate the cumulative flow observation to each other. Furthermore, the speeds at which observers travel influence to which points in space-time the characteristic waves can be drawn. Here, differences in the observer and characteristics wave speeds are beneficial. Therefore, it is desirable to have both relatively slow (e.g., trucks) and fast (e.g., passenger cars) vehicles that collect relative flow data, have observers that observe the opposite traffic flow, and combine stationary and moving observers.

There are multiple interesting future research directions. A first is a systematic (and analytical) extension of the effects of traffic properties, e.g., other FD shapes or higher order effects such as anticipation-behavior. Furthermore, based on the principles presented in this study, full methodologies and algorithms that exploit the informative value of the relative flow data can be developed. An important addition for this would be to apply the provided insights to information propagation over nodes.

Acknowledgements

This study was funded by the Netherlands Organisation for Scientific Research (NWO), grant-number: 022.005.030.

References

Amini, Z., Pedarsani, R., Skabardonis, A., Varaiya, P., 2016. Queue-length estimation using real-time traffic data. In: 2016 IEEE 19th International Conference on Intelligent Transportation Systems (ITSC), pp. 1476–1481.
Bhaskar, A., Chung, E., Dumont, A.-G., 2010. Fusing loop detector and probe vehicle data to estimate travel time statistics on signalized urban networks. Comput.-Aided Civil Infrastruct. Eng. 26 (6), 433–450.
Claudel, C.G., Bayen, A.M., 2008. Guaranteed bounds for traffic flow parameters estimation using mixed. Forty-Sixth Annu. Allerton Conf. 636–645.
Claudel, C.G., Bayen, A.M., 2010a. Lax-Hopf based incorporation of internal boundary conditions into Hamilton-Jacobi equation. Part I: theory. IEEE Trans. Autom. Control 55 (5), 1142–1157.
Claudel, C.G., Bayen, A.M., 2010b. Lax-Hopf based incorporation of internal boundary conditions into Hamilton-Jacobi equation. Part II: computational methods. IEEE Trans. Autom. Control 55 (5), 1158–1174.
Daganzo, C.F., 2005. A variational formulation of kinematic waves: basic theory and complex boundary conditions. Transport. Res. Part B: Methodol. 39 (2), 187–196.
Dervisoglu, G., Gomes, G., Kwon, J., Muralidhuran, A., Varaiya, P., Horowitz, R., 2009. Automatic calibration of the fundamental diagram and empirical observations on capacity. Transport. Res. Board 88th Annu. Meet. 1–13.
Fellendorf, M., Vortisch, P., 2001. Validation of the microscopic traffic flow model VISSIM in different real-world situations. Transport. Res. Board 80th Annu. Meet. 1–9.
Florin, R., Olariu, S., 2017. On a variant of the mobile observer method. IEEE Trans. Intell. Transp. Syst. 18 (2), 441–449.
Knoop, V.L., Daamen, W., 2017. Automatic fitting procedure for the fundamental diagram. Transport. B: Transp. Dynam. 5 (2), 129–144.
Laval, J.A., He, Z., Castrillon, F., 2012. Stochastic extension of Newells three-detector method. Transport. Res. Rec.: J. Transport. Res. Board 2315, 73–80.
Lighthill, M.J., Whitham, G.B., 1955. On kinematic waves. II.A Theory of traffic flow on long crowded roads. Proc. Roy. Soc. A: Math., Phys. Eng. Sci. 229 (1178), 317–345.
Makigami, Y., Newell, G.F., Rothery, R., 1971. Three-dimensional representation of traffic flow. Transport. Sci. 5 (3), 302–313.
Newell, G.F., 1993a. A simplified theory of kinematic waves in highway traffic, Part I: general theory. Transport. Res. Part B: Methodol. 27 (4), 281–287.
Newell, G.F., 1993b. A simplified theory of kinematic waves in highway traffic, Part II: queueing at freeway bottlenecks. Transport. Res. Part B: Methodol. 27 (4), 289–303.
Newell, G.F., 1993c. A simplified theory of kinematic waves in highway traffic, Part III: multi-destination flows. Transport. Res. Part B: Methodol. 27 (4), 305–313.
Redmill, K.A., Coifman, B., Mccord, M., Mishalani, R.G., 2011. Using transit or municipal vehicles as moving observer platforms for large scale collection of traffic and transportation system information. In: 14th International IEEE Conference on Intelligent Transportation Systems.
Richards, P.I., 1956. Shock waves on the highway. Oper. Res. 4 (1), 42–51.
Seo, T., Bayen, A.M., Kusakabe, T., Asakura, Y., 2017. Traffic state estimation on highway: a comprehensive survey. Annu. Rev. Control 43, 128–151.
Sun, Z., Jin, W.-L., Ritchie, S.G., 2017. Simultaneous estimation of states and parameters in Newell's simplified kinematic wave model with Eulerian and Lagrangian traffic data. Transport. Res. Part B: Methodol. 104, 106–122.
Treiber, M., Helbing, D., 2002. Reconstructing the spatio-temporal traffic dynamics from stationary detector data. Cooper. Transport. Dynam. 1, 3.1–3.24.
Van Erp, P.B.C., Knoop, V.L., Hoogendoorn, S.P., 2018a. Macroscopic traffic state estimation using relative flows from stationary and moving observers. Transport. Res. Part B: Methodol. 114, 281–299.
Van Erp, P.B.C., Thoen, S., Knoop, V.L., Hoogendoorn, S.P., 2018b. Estimating the fundamental diagram using moving observers. In: The 21st IEEE International Conference on Intelligent Transportation Systems, pp. 1–7.
Van Hinsbergen, C.P.I.J., Schreiter, T., Zuurbier, F.S., Van Lint, J.W.C., Van Zuylen, H.J., 2012. Localized extended Kalman filter for scalable real-time traffic state estimation. IEEE Trans. Intell. Transp. Syst. 13 (1), 385–394.
Van Lint, J.W.C., Hoogendoorn, S.P., 2015. A generic methodology to estimate vehicle accumulation on urban arterials by fusing vehicle counts and travel times. In: 94th AnnualMeeting of the Transportation Research Board. No. January.
Wang, Y., Papageorgiou, M., Feb 2005. Real-time freeway traffic state estimation based on extended Kalman filter: a general approach. Transport. Res. Part B: Methodol. 39 (2), 141–167.
Yperman, I., 2007. The Link Transmission Model for Dynamic Network Loading. Ph.D. thesis. Katholieke universiteit, Leuven.